Lab on a Chip

CRITICAL REVIEW

View Article Online
View Journal | View Issue

Cite this: *Lab Chip*, 2017, **17**, 2167

Progress of crystallization in microfluidic devices

Huan-huan Shi,[ab] Yan Xiao,[ab] Steven Ferguson,[c] Xin Huang,[ab] Na Wang[ab] and Hong-xun Hao *[ab]

Received 29th September 2016,
Accepted 23rd May 2017

DOI: 10.1039/c6lc01225f

rsc.li/loc

Microfluidic technology provides a unique environment for the investigation of crystallization processes at the nano or meso scale. The convenient operation and precise control of process parameters, at these scales of operation enabled by microfluidic devices, are attracting significant and increasing attention in the field of crystallization. In this paper, developments and applications of microfluidics in crystallization research including: crystal nucleation and growth, polymorph and cocrystal screening, preparation of nanocrystals, solubility and metastable zone determination, are summarized and discussed. The materials used in the construction and the structure of these microfluidic devices are also summarized and methods for measuring and modelling crystal nucleation and growth process as well as the enabling analytical methods are also briefly introduced. The low material consumption, high efficiency and precision of microfluidic crystallizations are of particular significance for active pharmaceutical ingredients, proteins, fine chemicals, and nanocrystals. Therefore, it is increasingly adopted as a mainstream technology in crystallization research and development.

Introduction

Operating parameters such as super-saturation, temperature, solvent composition, pH, *etc.* have significant effects on product quality in crystallization.[1–6] Interactions between these factors make it challenging to predict the crystallization behaviour, requiring significant empirical optimization. Therefore, new methods to clarify these interactions and minimize experimental efforts are sought.[7,8] Although, conventional approaches have been developed to optimize crystallization

[a] *National Engineering Research Center of Industrial Crystallization Technology, School of Chemical Engineering and Technology, Tianjin University, Tianjin 300072, China. E-mail: hongxunhao@tju.edu.cn; Fax: +86 22 27374971; Tel: +86 22 27405754*
[b] *Co-Innovation Center of Chemical Science and Engineering, Tianjin 300072, China*
[c] *School of Chemical and Bioprocess Engineering, University College Dublin, Dublin 4, Ireland*

Huanhuan Shi

Huanhuan Shi is a full-time doctoral graduate student at the School of Chemical Engineering and Technology at Tianjin University under the supervision of Prof. Hongxun Hao. Her research mainly focuses on microfluidic crystallization, including nucleation, polymorph screening and process optimization.

Yan Xiao

Yan Xiao is a PhD candidate, supervised by Prof. Jingkang Wang and Prof. Hongxun Hao, at the School of Chemical Engineering of Tianjin University, China. From October 2015 to September 2016, she was a visiting student under the supervision of Prof. Roger Davey and Dr. Thomas Vetter in the University of Manchester. She obtained her bachelor's degree in Chemical Engineering and Technology from Tianjin University in 2012. Her research interests mainly focus on crystal nucleation and pharmaceutical polymorphism. So far, she has published 4 peer-reviewed papers and applied 2 Chinese patents.

conditions, they are generally time-consuming and labor-intensive.[9] In addition to process design considerations, a number of fundamental shortcomings in the understanding of crystallization exists, particularly with respect to the nucleation theory.[10] For this reason, new experimental methods to investigate the mechanisms of nucleation and crystal growth in order to overcome limitations of traditional experimental approaches are also highly desirable.[11]

The emergence of microfluidic technology provides a new method for investigating crystallization. Compared to traditional methods, microfluidic devices offer a free-convection environment which is conducive to forming high-quality crystals, potentially simplifying future investigation and analysis.[12] Using microfluidic technology, crystallization experiments can be conveniently implemented under conditions of free interface diffusion and within nano-volumes.[13,14] Furthermore, advantages such as very large surface to volume ratios, microgravity, individual crystal confinement, excellent heat and mass transfer, and small volumes are realized.[15–17] As a result, it is possible to generate significantly higher supersaturations in microfluidic devices, than those encountered in conventional crystallizations. Crystal nucleation can be tightly controlled and manipulated, allowing single crystals with an ideal size and shape to be obtained.[18] Microfluidic technology also enables the application of high-throughput methods.[19] Micrograms of a material can be used to conduct a series of crystallization experiments under a variety of conditions, for example by changing the flow rate, temperature and solvent composition.[20–22] Suitable microfluidics, compatible with a number of crystallization applications,

Steven Ferguson

Steven Ferguson earned a B.E. (2008) and a PhD (2012) in Chemical Engineering at the University College Dublin in the Glennon Research Group. In 2012, he joined the Department of Chemical Engineering and Novartis-MIT CCM at the Massachusetts Institute of Technology, as a postdoctoral researcher under the supervision of Allan Myerson and Bernhardt Trout. Then he returned to join the faculty of Chemical & Bioprocess Engineering at the University College Dublin in 2015. His research focuses on continuous manufacturing, advanced separations, crystallization and reaction engineering to formulate novel processes for high value products in pharmaceuticals, biotechnology, drug delivery and nanotechnology.

Xin Huang

Dr. Xin Huang is a full-time associate research fellow of the School of Chemical Engineering and Technology at Tianjin University, China. He received his bachelor's degree in Applied Chemistry from Dalian University of Technology and his doctorate degree in Chemical Engineering from Tianjin University. His research interests lie in the area of industrial crystallization, including pharmaceuticals, oils & fats and nano-materials. He has published more than 10 peer-reviewed publications and applied 3 Chinese patents.

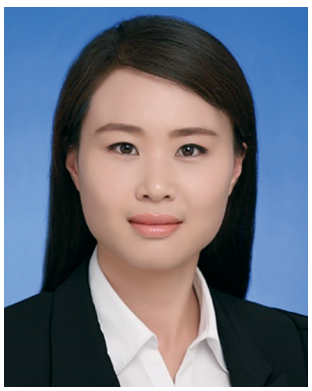

Wang Na

Wang Na is a full-time doctoral graduate student at the School of Chemical Engineering and Technology at Tianjin University, China. Her research interests lie in the area of industrial crystallization and separation of isomeric compounds by co-crystallization.

Hong-Xun Hao

Hong-Xun Hao is a full professor of the School of Chemical Engineering and Technology at Tianjin University. He obtained his Ph.D. from Tianjin University in 2003. He was a visiting scholar at the University College London (the UK) in 2005 and a senior research fellow at the University College Dublin (Ireland) from 2009 to 2011. His research interests mainly include the development of novel crystalline materials, crystallization technology, nanocrystalline materials, and microfluidic crystallization. He has published more than 100 publications in peer-reviewed journals and applied for more than 40 patents.

continue to mature and have been demonstrated in the crystallization of proteins,[23–25] pharmaceuticals,[26,27] and nanocrystals.[28,29]

While crystallization in microfluidics is a promising technology, more work is needed to address its current limitations, primarily: propensity for clogging, high pressure drops, cost and operability issues for wider adoption, especially for industrial uses. This work aims to promote the development and application of new microfluidic technology in crystallization processes. The state of art and the future scope of this research field are summarized and discussed. The materials and structures that are used for fabricating microfluidic setups are described. Their advantages and disadvantages are enumerated. The applications of microfluidics in different aspects of crystallization processes, including crystal nucleation, growth, polymorph screening, nanocrystals preparation, *etc.*, are summarized and illustrated using examples. Finally, the methods and models proposed to obtain data to investigate the fundamental mechanisms of crystallization are also discussed.

Materials and structure of microfluidic devices for crystallization

To satisfy the requirements for microfluidic crystallization, a variety of materials and channel structures have been developed.

Materials for fabrication of microfluidic devices for crystallization

A number substrates have been applied in the fabrication of microfluidic devices for crystallization, and each presents its own advantages and limitations. Substrate choice determines the surface characteristics of the microfluidic channels, which can influence crystallization and prevalence of fouling and clogging within channels, in addition to heat transfer of particular relevance in cooling crystallizations. Chemical compatibility with solvents and solutes should be considered in the selection of suitable materials for construction. The rate of formation of droplets, slugs and hydrodynamic stability of immiscible liquid–liquid phases can also be influenced by material selection. Hence, selecting appropriate materials is crucial in fabricating microfluidic devices for crystallization research. Materials used for fabricating microfluidic devices can be classified into three categories:[30] (i) inorganic materials: primarily glass and silicon; (ii) elastomers and plastics: most commonly PDMS, PMMA, PVC, COC and Teflon PFA/FEP; and (iii) hybrid and composite materials: for example PDMS/glass and COC–PDMS.

Glass and silicon. Glass and silicon are the earliest materials used in microfluidics. The optical transparency of glass is convenient for direct observation *via* microscopy. In addition, it is highly biologically compatible and its surface modification is relatively straightforward. Roughness of the glass channel surface is known to affect the performance of microfluidic devices, which results in larger flow resistance, causing significant changes in the fluid velocity along the channel. Thermal fusion bonding is widely used for sealing glass microfluidic channels but this temperature pretreatment will influence the performance of channels. For this reason, the glass surface often needs to be polished and cleaned. Che-Hsin Lin *et al.* developed a two-step baking process and a shorter thermal bonding process to address these problems.[31] An intermediate layer is found to be an essential prerequisite for successful glass–glass bonding.[32,33] However, the fabrication procedure is complex and expensive. Recently, simple and low-cost microfluidic devices based on microscope glass slides and glass capillaries were reported to be able to overcome these disadvantages.[34,35] Silicon has some useful attributes such as insulation and resistance to organic solvents[36] and mechanical stress. Due to its surface properties, silicon has extensive applications in protein crystallization. For example, patterned silicon wafer surfaces promote selective nucleation.[37] However, silicon is opaque, fragile, expensive and has complex surface chemistry, which limits its application.

PDMS. PDMS is an inexpensive material, has excellent gas/water permeability and good optical properties, which have made it one of the most popular substrates used in microfluidics.[38–41] However, microfluidic devices made from PDMS have poor solvent compatibility, a major limitation in microfluidic crystallization of organic compounds. Lee *et al.*[42] investigated the compatibility of PDMS with organic solvents from three aspects: swelling, partitioning of solutes and dissolution of PDMS oligomers and found that swelling was found to be the most impactful to performance and the compatibility of PDMS was correlated with solvent. Solvents that swelled PDMS the least included water, nitromethane, dimethyl sulfoxide, ethylene glycol, perfluorotributylamine, perfluorodecalin, acetonitrile, and propylene carbonate. Solvents that swelled PDMS the most were diisopropylamine, triethylamine, pentane, and xylenes. For the fabrication of microfluidic devices, the low surface free energy of PDMS makes it easy to release from molds or combined with other materials.[43] As such, PDMS is usually combined with other materials, such as glass or silicon, to solve the problems of swelling and limited solvent compatibility. Abate *et al.* described a glass coating for PDMS channels with a solvent-resistant, glass-like substance using sol–gel methods.[44] Domenichini *et al.* presented the fabrication of layered PDMS/PFPE microfluidic devices with good solvent compatibility and valve functionality.[45]

PMMA. Because of its high optical transmission, good solvent and chemical compatibility, high stability and well-characterized molding parameters, PMMA has also been widely used in the development of thermoplastic microfluidic systems.[46] A. Muck and co-workers described a simple, user-friendly and effective method for the fabrication of PMMA microchips using atmospheric molding.[47] An SU-8-based stamp was used to fabricate PMMA microfluidic devices by hot embossing lithography.[48] SU-8 was chosen because of its

excellent coating, planarization and processing properties as well as mechanical and chemical stability.[49] A. Toossi *et al.* successfully developed an innovative method of PMMA microfluidics bonding using commercial microwave ovens.[50] Setting the temperature above the glass-transition point within a certain range, PMMA will become soft and flexible and hence can be heated selectively and efficiently to minimize time and energy requirements for fabrication of PMMA microfluidic devices. PMMA can be modified to enable resistance to acid, alkali, and organic solvents. Subramanian *et al.* developed an approach to modify the wettability of the surface of PMMA,[51] which was found to have similar results with some other materials (PC and COC). Despite these developments, after long-term exposure to organic solvents, the PMMA channels are prone to transverse rupture and swelling, resulting in local deformation and rough surfaces.

Hybrid and composite materials. As each of the materials currently used for fabricating microfluidic devices has its own limitations, hybrid and composite materials are an attractive solution, and the subject of on-going research efforts. By combining several materials, improved functionality of microfluidic devices can be achieved. For crystallization processes, hybrid and composite materials of PDMS with other materials are mainly utilized. Sealing channels in PDMS is simpler than that in glass, silicon and thermoplastics since PDMS can be sealed with itself or other materials without distorting channels geometry.[52–57]

An automatic compact disk-like microfluidic device based on capillary effects and centrifugal force was presented by Li *et al.*[58] and Wang *et al.*[59] It was a PDMS/glass hybrid microfluidic device and was reversibly bonded by a PDMS sheet containing channels and chambers with a glass wafer. This device was successfully used for high-throughput nanoliter-scale protein crystallization screening. It had a simple structure, picoliter accuracy and produced negligible sample waste. Yu *et al.* proposed another PDMS/glass system for protein crystallization.[60] The high gas permeability of PDMS, often a disadvantage of PDMS, was harnessed in this device. Multilayer soft lithography was used and PDMS film thickness was purposely designed to meet the experimental requirements for in-process evaporation. Another example is the microfluidic device which was fabricated by using PDMS molded on a master silicon wafer using a negative photoresist (SU-8, Microchem).[61] In order to assure all channel walls are composed of the same materials, the PDMS-molded channels were sealed with a silicon wafer which was previously covered by a thin and cured PDMS layer. A nanofluidic chip, composed of an upper PDMS cover and a polycarbonate substrate with nanochannels,[62] a PDMS–hydrogel hybrid chip, PDMS–ZnO composites with an *in situ* temperature sensor[30] and a COC–PDMS microfluidic device[63] have also been reported.

Other materials. Use of simple junction geometries and tubing, for example T-junctions, Y-junctions and cross-shaped junctions, can enable the utilization of additional materials such as PEEK with PVC or Teflon tubing.[64–67] Cleaning these kinds of devices is more convenient and they are compatible with most solvents except for concentrated acids (such as sulphuric acid and nitric acid). These simple configurations often utilize relatively large diameter channels with immiscible dispersed phase droplets creating the microvolume for crystallization. Droplet size can be controlled by channel dimensions and flow rates. Concentration and composition of droplets can also be adjusted by using programmable multichannel syringe pumps or controlling the relative flow rates.[68] Compared with PMMA or PDMS, it is more convenient for junctions to control the system temperature even though this kind of device has no heating element. For instance, the tube is immersed in a water bath at a desired temperature, which also eliminates the cumbersome process of setup fabrication.[67]

Types of microfluidic devices for crystallization

Microfluidic devices for crystallization can be divided into four main categories: continuous flow microfluidics, droplet-based microfluidics, valve-based microfluidics and digital microfluidics.[69]

Generally speaking, microfluidic continuous crystallizations (Fig. 1)[70] have predetermined residence times, rapid mixing and excellent mass and heat transfer. Compared with conventional crystallization, higher supersaturation levels and hence smaller crystal sizes can be achieved by increasing the nucleation rate. Reduced supersaturation gradients in microfluidics also enable a more homogenous nucleation hence a smaller mean crystal size and a more mono-disperse crystal size distribution to be achieved at a given level of supersaturation. Su *et al.* synthesized inorganic ($BaSO_4$) and organic (docosapentaenoic acid) nanoparticles in reactive and anti-solvent crystallization, using a continuous microfluidic-based emulsion crystallization.[71] Jasch *et al.* proposed a microfluidic approach for a continuous crystallization of drug carrier nanoparticles. This method provides an alternate to melt homogenization *via* high-pressure in the preparation of solid lipid nanoparticle suspensions.[72] Dev *et al.* presented a simplified method for nanosized drug formulation under a

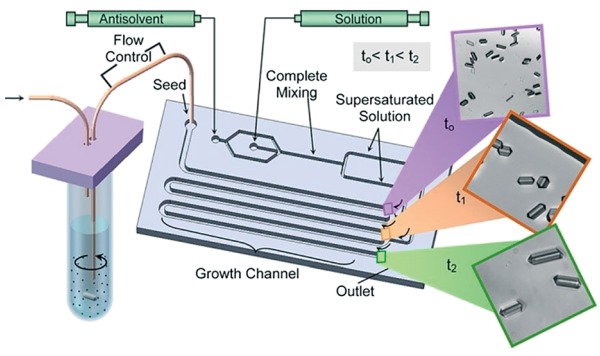

Fig. 1 Schematic of microfluidic continuous crystallization. Reproduced from ref. 70 with permission from the American Chemical Society.

microfluidic continuous flow.[27] Ultrafine drug nanoparticles were produced on a rapidly rotating surface where rapid nucleation and controlled growth was achieved in an intense micro-mixing environment. The obtained product had a controlled size, narrow size distribution and high dissolution rate in the absence of polymer additives. Sultana & Jensen designed a continuous seeded microfluidic crystallization approach,[70] where the growth kinetics of α, β, and γ-forms of glycine were determined, and the impact of impurity on morphology was investigated. This approach could also be utilized to study the effect of additives on the crystal habit, a factor that can strongly impact downstream process performance and that of the solid product itself. The prevailing laminar flow conditions could produce self-alignment of high-aspect ratio crystals. However, despite the successful continuous microfluidic crystallization demonstrations, fouling and blocking of channels in addition to agglomeration and sedimentation of crystals remain as the major challenges. Avoiding contact between crystals, a supersaturated solution and the channel walls can maintain crystal quality and limit clogging. Surface modification can also aid in overcoming these issues. Another method is to enhance the mixing, which can be achieved by using several types of mixers, such as T-mixers, grid mixers, and jet mixers.[73]

In droplet-based microfluidic crystallization processes (Fig. 2 (ref. 61)), the supersaturated solution is confined in a dispersed droplet phase, within an immiscible carrier fluid.[74] The mean size and poly-dispersity of droplet distributions in microfluidic devices can be tightly controlled compared to traditional crystallization approaches. Droplet-based microfluidic crystallizations are mainly used to investigate nucleation rates through measurement of the number of crystals inside a droplet (of known volume) *vs.* time, at a range of supersaturations and process conditions. The small volumes enable an accurate quantifiable measurement of the probabilistic nature of primary nucleation which can be highly challenging to observe using alternate approaches[61,75] Furthermore, droplet-based microfluidic crystallization enables rapid collection of large amounts of data in investigating kinetics and screening crystallization conditions. This method was also used for preparing nanoparticles[28] and screening solubility diagrams.[76] Compared to conventional experimental configurations, droplet-based microfluidic crystallization can produce narrower crystal size distributions.[67,77] Both the mean crystal size and the maximum possible crystal size can be controlled by adjusting the droplet size and initial supersaturation.[78] The generation of droplets depends on the selection of suitable immiscible phases and the channel geometry (including T-junction and flow focusing).[79] If a stable multiphase dispersion can be obtained, the monodisperse droplets can act as miniature and independent crystallizers.[80,81]

An example of a valve-based microfluidic crystallization device is shown in Fig. 3.[82] In these configuration, reagents are injected into the microfluidic device *via* opening or closing of valves. It has been applied to investigate crystallization *via* a free interface diffusion approach under parallel control within identical units. Lau *et al.* developed a microfluidic device with integrated microvalves.[83] The microvalves could generate single droplets at defined times with precise and independent control over the composition, size, and spacing.[83] Perry *et al.*[82] reported an integrated microfluidic chip where the pneumatic valves drove the flow by limiting the maximum achievable pressure supplied to the valves. When the viscosity of the fluid was low, isolation valves were used to control the fluid flow instead of injection valves.[82] Subsequently, Li *et al.*, utilized the valve-based microfluidic device to screen crystallization conditions for a protein.[24] The loading and mixing of samples was controlled through the opening and closing a series of pneumatic valves.

Digital microfluidics (Fig. 4 (ref. 84)) is a promising technology for liquid handling, enabling the control of individual droplets.[23,85] In contrast to channel microfluidics with pumps, valves or mechanical mixers, digital microfluidics utilizes force generated by electrowetting-on-dielectric on an array of electrodes with a hydrophobic coat to control the flow. Generally, it can achieve the droplet based operations including merging, dispersing from sample/reagent reservoirs,

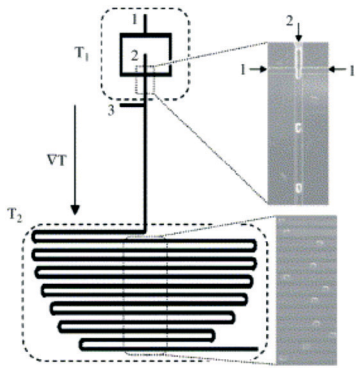

Fig. 2 Schematic of a droplet-based microfluidic device for crystallization. Reproduced from ref. 61 with permission from Elsevier.

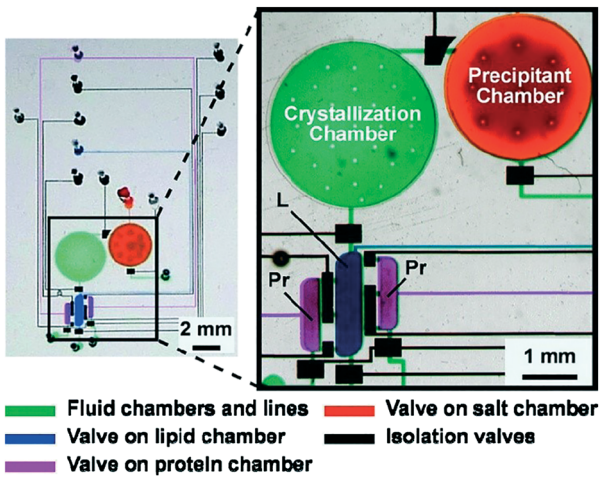

Fig. 3 Optical micrograph of a valve-based microfluidic device, in which the fluids are controlled by various valves. Reproduced from ref. 82 with permission from the American Chemical Society.

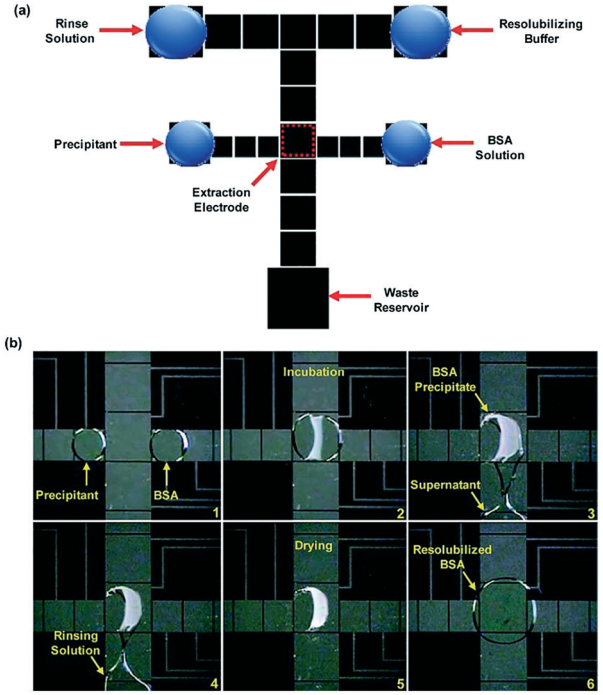

Fig. 4 (a) Schematic of a digital microfluidic device. (b) The procedures depicted by a movie. Reproduced from ref. 84 with permission from the American Chemical Society.

transferring, mixing and splitting through unique force.[86–88] Although droplet-based microfluidics limits the interaction between the individual droplets, it can deal with many reagents simultaneously and individually,[89–91] which is quite useful for proteomics. Digital microfluidics can also be used to extract and purify proteins.[84] Another advantage of digital microfluidics over channel-based microfluidics is that clogging should not occur when transporting and handling solid particles.[86] However, cross-contamination and solute adsorption in 2D digital microfluidics systems presented challenges for the development of digital microfluidics. A number of strategies have been worked out to solve these problems. Hong *et al.* developed a three-dimensional digital microfluidics platform where temperature-controlled chemical reactions can be conducted.[92] In 2D or 3D digital microfluidics, the direct contact of droplets with the solid surface though the droplets' movement can lead to another limitation of this technique. Droplet lift-off methods are proposed to tackle this issue[93–95] and an immiscible fluid system is introduced.[36,96,97] In addition, there are several other challenges in digital microfluidics: sample preparation, discrepancies between droplet volumes, compatibility of real samples with effective actuation on the chip, limited droplet generation throughput and fabrication cost.[98] Nevertheless, digital microfluidics could have significant potential in nanoparticle synthesis.

Channel structures

The channel structure of microfluidic devices has a significant impact on crystal nucleation and growth. Improper design will result in blocking of the channels during the formation of crystals. The channel design should comply with the experiment requirements such as: chemical compatibility and the ability to generate and maintain the desired microfluidic flow profile.

In terms of droplet-based microfluidics, the generation and control of monodisperse droplets are important for investigating crystallization. Droplets are normally generated by four kinds of channel structures: capillaries, flow-focusing, Y- and T-junctions (shown in Fig. 5).[79,99,100] The capillary structure is preferentially used for spherical crystallization which requires a highly monodisperse distribution of the droplet size.[34] It has been shown that these attributes of the capillary structure enable remarkable control of size, shape and size distribution of spherical crystals. Leon *et al.* successfully adopted a capillary-based microfluidic device for simultaneous spherical crystallization of drugs and excipients.[101] However, the capillary-based microfluidics is not suitable for reactive or anti-solvent crystallization which requires rapid and effective mixing. Flow-focusing structures and T-junctions are the most popular droplet-based microfluidic geometries[61,102] since uniform droplets can be generated simply by adjusting the relative velocity and viscosity of the medium used. There are several modifications for these structures. Teychené & Biscans[103] presented a droplet-based microfluidic method (flow-focusing) with 64 parallel channels, combined with two Peltier elements to investigate crystallization at various temperatures. Ildefonso *et al.* developed a microfluidic device to determine the metastable zone width of protein crystallization processes.[104] This modified structure can also be used for generating droplets with various concentrations by adjusting the relative flow rates of incoming streams.[105] Zheng *et al.*[14] developed a microfluidic device for screening protein crystallization conditions. In this device, the solutions are injected so that the composition of each microfluidic crystallization droplets can be varied

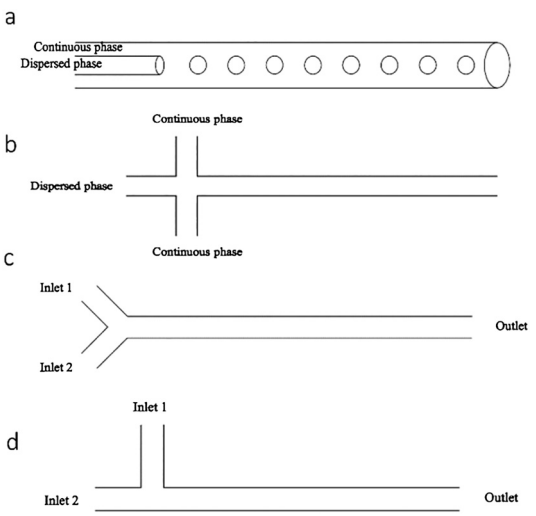

Fig. 5 Design of droplet generation structures in microfluidics based on (a) capillaries; (b) flow-focusing; (c) Y-junctions; and (d) T-junctions.

continuously and rapidly, with each drop representing a unique set of crystallization conditions. Subsequently, Zheng *et al.* developed another device to evaluate the protein crystallization conditions.[106] Moreover, premixing before droplet formation was successfully achieved by modifying the structure.[107] It ensures uniform mixing of components when forming droplets. In Y-junctions, the droplet size is more sensitive to the processing conditions which have been found to result in a large variation of the droplet size.[100] Vitry *et al.* utilized a microfluidic system with a Y-junction to study reactive crystallization by coalescing droplets.[108] However, Y-junction type microfluidic devices are not well suited to anti-solvent crystallization conducted with laminar flows. Slow flowing supersaturated solutions and crystals along the channel walls are prone to adherence to walls and surface fouling, leading to channel blockage. Bhamidi described a modified device in their work to minimize crystal adhesion by directing the supersaturated crystallizing solution to the center of the microchannel.[109]

Well-based microfluidics and microfluidic channel geometries have also been demonstrated. The well based microfluidics shown in Fig. 6 was developed for screening of polymorphs[110] and cocrystals[111] of active pharmaceutical ingredients. On the other hand, microfluidic channel geometries are often used for protein crystallization.[112] A nanowell array chip is a multilayer design using inexpensive materials such as silicon and PDMS. Generally speaking, the nanowell arrays have two geometries: round-well and square-well.[113] In the nanowell device, each nanowell is separated from each other. Hence a large number of trials can be carried out individually in a single nanowell array slide with nano-volume of solutions per trial. Meanwhile, the confined space is conducive to generating suitable crystals. Finally, crystal arrays are formed for high quality analysis. And the amount of nanowalls in this system is easy to adjust. An actuated nanowell array chip shows its superiority in protein crystallization.[114] For instance, by virtue of the use of valves, solutions with a concentration gradient are loaded and isolated from each other in nanowells. It is convenient to observe crystals and screen complex multidimensional crystallization under different conditions.

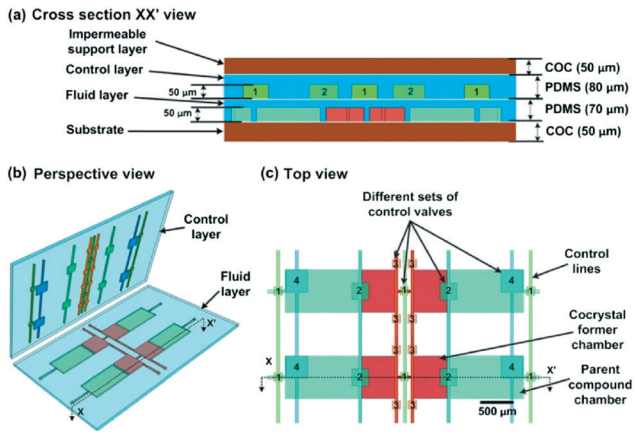

Fig. 6 (a)–(c) are cross-section view, perspective view and top view of microfluidic crystallization wells, respectively. Reproduced from ref. 111 with permission from the American Chemical Society.

Another kind of microfluidic device, the Microlytic Crystal Former,[115] is usually used for proteins to produce concentration gradients by free diffusion. There are three main types: CF-HT2, CF-O and CF-XL, which are composed of 96 microchannels, 16 microchannels and 16 larger microchannels than CF-O's, respectively. High output, simple to use and automatable, low protein consumption, and direct crystal harvesting are the advantages of the Microlytic Crystal Former. However, several limitations can be encountered: bubbles and gradient dissipation due to sealing issues, dehydration if the cryoprotectant is not timely applied during harvesting, disturbance of the adjacent channel by incomplete film cutting, and adherence of crystals to the sealing film upon removal.

Another structure, the SlipChip, which is usually used for protein crystallization, has two categories: free interface diffusion SlipChip and composite SlipChip, which is capable of implementing free interface diffusion and microbatch crystallization at the same time.[116] SlipChip mainly relies on the relative sliding of two plates to realize the connection between protein wells and precipitant wells, and then the solutions can be mixed to proceed independent crystallization under different conditions with a low consumption of the sample. However, SlipChip also has some shortcomings. For instance, when slipping the plates, the residual solutions on plates may cause cross-contamination. To solve this problem, it is feasible to change the contact angle between solutions and plates. The question then is that a solution becomes unstable with larger angles, which requires modifying the surface characteristics of the SlipChip. Compared with free interface diffusion SlipChip, the composite SlipChip is more efficient to screen crystallizations and can be used to investigate new conditions.

Applications of microfluidics in crystallization

Microfluidic systems can access experimental conditions not available within bulk crystallizations and hence a wider range of product qualities. Furthermore, they have potential to produce extremely reproducible particle properties and enable rapid collection of data to quantify crystal nucleation and growth rates with small amounts of the material. Crystal nucleation and growth can be decoupled and investigated independently in microfluidic devices.[107,117] For these reasons, microfluidics is increasingly applied to efficiently investigate and optimize crystallization conditions.[59,118,119] It has also been demonstrated that crystals obtained in droplet-based microfluidics have a narrower size distribution than those prepared with bulk crystallization.[120] In addition, the droplet-based microfluidics also has some advantages in nanocrystals synthesis, solubility determination and polymorph screening.[105,110,121,122]

Nucleation and crystal growth

The highly uniform crystallization environment afforded by microfluidic crystallization is useful in the study of crystallization kinetic parameters. More homogeneous nucleation events can be realized across a wider range of supersaturations. Therefore, nucleation rates can be estimated more accurately by using microfluidic devices.[102] Batch methods (*e.g.* crystal 16) have been used to investigate nucleation also. But only a number of limited parallel experiments can be performed simultaneously in small batch crystallizers. However, hundreds of uniform droplets can be stored and act as independent crystallizers in droplet-based microfluidic devices.[103] Accurate collection of population statistics for nucleation, which are lost in larger vessels, can be measured and secondary (solid catalysed) nucleation is also largely suppressed aiding in the study of primary nucleation from a solution. Furthermore, microfluidics can provide a more intuitive observation of crystal nucleation and growth processes through direct droplet observation using a simple microscope configuration (shown in Fig. 7).[123]

Sanjoh and co-workers investigated spatiotemporal nucleation and post-nucleation growth of protein crystals in a microfluidic silicon device.[37] These two processes were shown to be dependent on the electrical properties of the Si surface layer. Based on this observation, a possible mechanism of heterogeneous nucleation and growth of protein crystals was proposed and discussed. In 2007, Shim *et al.* used a Phase Chip, in which droplets of a protein solution could be stored in individual wells under 1000 different conditions, to decouple nucleation and growth of protein crystals.[107] In this method, stable protein solutions were formulated first. Then supersaturation dialysis was used to suppress supersaturation to levels that growth would dominate. After several recrystallization cycles, defected crystals were eliminated by selective dissolving and growing of different crystals. Finally, larger crystals were obtained by using dialysis to reduce concentrations of protein and salt, which will result in dissolution of small crystals and growth of larger crystals. Properly designed microfluidic channels can also decouple the nucleation and growth processes.[117] It has been demonstrated that the depth of channels could affect the crystal nucleation and growth processes: nucleation dominates in deep channels while growth dominates in shallow channels.

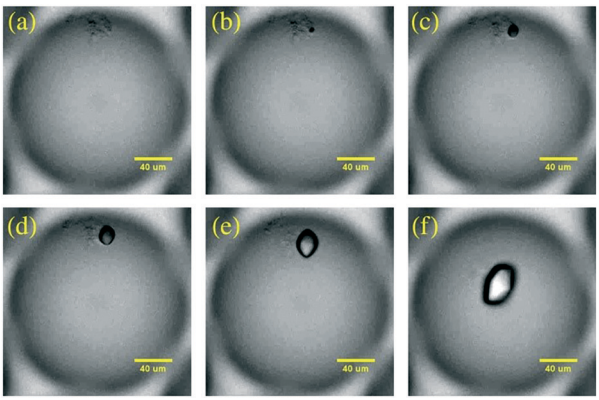

Fig. 7 Nucleation and growth of a protein crystal in a droplet-based microfluidic device at different time. From (a) to (f) at t = 0 s, 15 s, 45 s, 75 s, 120 s, 300 s, respectively. Reproduced from ref. 123 with permission from the American Chemical Society.

While microfluidics can be used for nucleation and growth, it is more often used as a tool to study nucleation. Nucleation itself can be subdivided into a number of broad mechanistic categories: primary nucleation and secondary nucleation. In traditional methods and most commonly observed solution crystallizations in the lab or industry, primary (heterogeneous nucleation) generates the initial solid phase followed by secondary nucleation which generates much of the crystals in the resulting population. As such, the induction time or MSZW is indicative of primary nucleation, but the total number cannot be used to characterize the nucleation rate. Primary nucleation can be further subdivided into homogenous and heterogeneous nucleation, where the energy barrier for (homogenous) nucleation is influenced by impurities within the system, which are almost inevitably introduced into the investigated systems and can increase or decrease the observed rate. Microfluidics can be used to investigate homogeneous nucleation since impurities can be eliminated by using the microfluidics technology.[124] Usually, in microfluidic devices, only an ultra-small amount of the material is needed, which reduces the probability of impurities existing in the droplets. For example, if the number of droplets is large enough and the volume of the droplets is sufficiently small, homogeneous nucleation will be achieved.[70] Valve-based microfluidic systems, proposed by Lau *et al.*,[83] have been applied for large-scale screening of homogeneous assays by free interface diffusion in crystallization processes. Recently, a liquid-filled microchannel was developed to investigate homogeneous nucleation.[102,124] It enabled nucleation rates to be estimated more accurately,[125,126] from the relationship between the probability distribution of crystals appearing in droplets and time.[61,67]

Nucleation rates have been investigated with low prediction errors by using microfluidics technology.[75,103,127–129] Recently, heterogeneous nucleation of lysozyme was investigated in droplet-based microfluidics. How heterogeneous nucleation influenced the determination of thermodynamic and kinetic factors was also discussed.[130] Rossi *et al.* determined the primary nucleation kinetics for adipic acid using droplet methods under stagnant and flow conditions.[131] Results showed heterogeneous nucleation represents the adipic acid nucleation mechanism and that primary nucleation could be enhanced under flow conditions. Recently, a gas-segmented flow was used in a microfluidic device to study nucleation of APIs.[132] The estimated parameters were found to be consistent with the literature values, and nucleation rates increased more sharply than what would be predicted by the classical nucleation theory. The use of microfluidics has been demonstrated to allow nucleation kinetics of a variety of proteins and APIs to be determined rapidly, accurately, and with great sensitivity. These findings pave the way for new designs and further refinement of microfluidic devices for this application.

Microfluidics technology has also been used to produce spherulitic crystals or crystals with an extremely narrow size distribution by controlling the nucleation and growth rates of crystals.[133–136] The droplet-based microfluidic devices have shown their advantages in the production of spherical crystals.[101,103,137,138] This technology provides important alternative methods for the fabrication of monodisperse spherical agglomerations of pharmaceutical formulations.

Polymorph and cocrystal screening

Since only limited capabilities in crystal structure prediction have been demonstrated, form screening still represents the gold standard in the discovery of new crystalline forms for a given compound. Compared to the current standard approach, microfluidic screening methods offer a number of significant advantages. The micro-fluidic environment emphasizes primary nucleation rather than secondary nucleation, which will favour the discovery of a larger variety of polymorphs and co-crystals in some configurations. Furthermore, at smaller volumes, the inherent stochasticity of nucleation has a larger significance with low probability of nucleation of a second form in a droplet or a small volume environment, meaning that even highly unstable forms within a microfluidic environment can be persistent and observable. Finally, the ability of microfluidic devices to make direct observations optically and *via* spectroscopy to characterize new polymorphs and cocrystal forms is also highly advantageous. In addition to microfluidics, crystallization in confined environments can also be used to generate constrained volumes for polymorph and cocrystal screening. For example, self-assembled monolayers have been successfully used to perform a large number of polymorph/co-crystal experiments outside microfluidic flow devices.[139–142] Confinement within mesoporous microvolumes, hydrogels and polymers can also generate and stabilize metastable crystal forms.[143,144] However, difficulty in characterization makes them less suited to screening than microfluidics.

Polymorphs. Polymorphic forms are one of the key criteria that characterizes the quality of crystalline products. Different polymorphs of the same compound may exhibit varied physical and chemical properties. As such, polymorphs can have profound effect on the bioavailability and chemical stability of the product, qualities of particular interest in pharmaceutical compounds. Therefore, polymorph screening and selection of appropriate polymorphs are crucial steps for drug development. In most cases, the most stable thermodynamic form is sought for active pharmaceutical ingredients (APIs). However, comprehensive identification and characterization of all polymorphs has important intellectual property and risk mitigation implications and is an area where microfluidics could see significant industrial penetration. Screening of polymorphs is labour intensive because many factors, such as solvent composition, temperature, concentration, supersaturation, solution impurity profile, and the presence of doped soluble components, can affect the formation of different polymorphs.[145]

Recently, progress has been made in microfluidics polymorph investigation and screening. Control of the crystal polymorph in microfluidics led to the discovery of new polymorphic forms which were never observed through conventional methods.[146] Ji *et al.* demonstrated that a 28 kDa EP protein concentration gradient played an important role in calcium carbonate polymorph selection. The consumption of calcium chloride and sodium carbonate solutions was about 5 μl. Due to the small dimension of the microfluidic device, concentration gradients were generated stably based on diffusion. In the presence of the 28 kDa EP protein, both hollow vaterite and rhombohedral (and layered) calcite crystals were observed under both positive and negative controls in the microfluidic devices while only rhombohedral calcite crystals were formed in bulk systems using traditional methods. Geneviciute *et al.* reported polymorph control in inorganic crystal systems at a microdroplet liquid interface.[147] In this study, the average volume of a droplet was around 0.5 nL in the ~200 μL immiscible phase. Anionic, neutral and cationic surfactants as well as different temperatures were used to investigate the impact on crystals habits. It was found that different surfactants and temperatures would result in different crystal habits. Additives were also used to screen crystal forms. Concomitant polymorphs were also observed. Two different crystal forms were observed as shown in Fig. 8. These results showed a novel method for investigating polymorphism at the liquid–liquid interface. It has been known that lysozyme has two crystal habits,[148] and M. Ildefonso *et al.* explored its polymorphism *via* microfluidics. By changing the temperature, different crystal habits were obtained. Results showed that when the temperature was raised to a certain value, crystals with a sea urchin-like habit dissolved and the tetragonal crystals were stable and continued to grow.[104] The confined space in droplets (250 nL) increased the existence of metastable crystals because of higher supersaturation. In addition, a single crystal was also conducive to stabilize metastable crystals.

Antisolvent crystallization in microfluidics has also been used for screening of polymorphs.[109,110] Thorson *et al.*

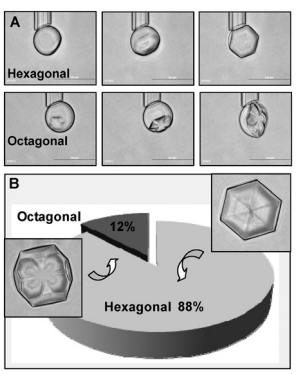

Fig. 8 (A) Formation of two different crystal forms depicted by video micrographs. (B) The fraction of crystal habits found in experiments. Reproduced from ref. 147 with permission from the American Chemical Society.

screened polymorphs by precisely controlling the volumetric ratios between solvents and antisolvents in a 48-well chip. Moreover, different solvents were selected for the microfluidic devices. Solvents and antisolvents were mixed by gradual diffusion, avoiding excessive local supersaturation. A microscope was used to monitor crystals and Raman spectroscopy was also used to analyze crystal products. Bhamidi and co-workers utilized slow diffusion at the laminar flow interface, where the center stream was the solutions and the side streams were the antisolvents. The experiments were conducted by varying the flow rate and concentration of the antisolvent, respectively, or both to generate complex concentration gradients along the channels. Polymorphic forms were observed by off-line Raman microscopy. This method allowed the analysis of polymorph selectivity prior to the occurrence of metastable crystal transformation. Compared to conventional screening approaches, polymorph screening in microfluidic devices can be carried out with limited raw materials, which greatly minimizes the consumption of expensive materials. It is also convenient for screening of polymorphs at different ratios of solvents and anti-solvents simultaneously in a single microfluidic device.

Cocrystals. Cocrystals are solid phases where two or more neutral molecules exist in a crystal lattice.[149] While solvents and hydrates also meet this criterion, the term co-crystal is often considered to only describe solids where the individual constituent molecules in the co-crystal lattice are solid outside the solution at ambient conditions. The design of cocrystals has shown great potential to develop materials with desirable properties.[150] In pharmaceuticals, cocrystals can be prepared to improve API physicochemical characteristics, such as stability, solubility, bioavailability, *etc.*[151–153] Conventional cocrystal preparation methods including evaporation, reaction, cooling crystallization, grinding, ultrasonic and supercritical fluid methods have been thoroughly discussed and reviewed.[154,155] However, the procedures are often complicated and cannot be applied to industrial production directly. Meanwhile, the polymorphism of cocrystals has rarely been investigated. Thus, more accurate and reliable technologies to screen and identify cocrystals would be beneficial in both industrial and academic environments.[156–158]

With adoption of microfluidics, cocrystals could be screened at the early stages of drug development despite the availability of only small quantities of materials. In such microfluidic configurations, cocrystallization experiments can be implemented under different conditions simultaneously. X-ray diffraction and Raman spectroscopy can be conducted on-chip to monitor and screen solid forms. Goyal *et al.* described a microfluidic approach to screen cocrystals of APIs.[111] The platform could conduct experiments under 48 unique combinational conditions on-chip and enables mixing the solutions *via* free interface diffusion. And each condition just consumes about 90 nL of a solution and 48 conditions require 240 μg of pharmaceutical parent compounds (PCs) totally, which is much lower than those used in the conventional methods. The solids were observed periodically by using an optical microscope and crossed polarizers. Cocrystals located in different chambers were analyzed rapidly using on-line Raman spectroscopy. Subsequently, Goyal *et al.* utilized and validated an evaporation-based microfluidic device for screening salts of APIs,[159] and more recently co-crystals.[160] The microfluidic device with a 24-well array required around 200 nL per well and consumed less than 10 μg of PCs per condition. The screening was based on evaporation of the solvent. To control the crystallization, the evaporation rate of the solvent was controlled at 2–15 nL h^{-1}. By changing the evaporation rates of the solvents, crystalline solids were formed in a 24-well array, and the crystal size could be controlled on-chip. On-chip Raman analysis identified six different salts for each model compound, tamoxifen and ephedrine. Horstman *et al.* employed a 72-well array microfluidic platform for screening of seeding conditions of cocrystals.[161] It was easy to operate and could simplify the microseeding process with about 5 μg per well of PCs. In this study, four systems were investigated by the microseeding approach, and the seed dilution ratio between the API solution and the microseed solution was investigated to obtain isolated crystals for collecting X-ray data. X-ray data at room temperature were used to determine the structure of the cocrystals. And the comparison results between seeded and unseeded experiments are shown in Fig. 9. It was also shown that better outcomes could be obtained if temperature control was applied to the system.[161]

Preparation of nanocrystals

Nanoparticle precipitation approaches are usually broadly categorized as "top–down" or "bottom–up". A large number of approaches within each of three categories are reported in the literature[162,163] However, the conventional methods have some disadvantages. For example, the top–down method is energy-consuming and might introduce impurities into the system. The bottom–up method has difficulty in controlling the crystal size and polymorphs because of intense mixing. Also, these methods are not suitable for organic nanocrystals with thermal instability and weak mechanical characteristics. Microfluidic nanoprecipitation/crystallization approaches offers exclusively "bottom–up" formation of nano-particles from solution. To fabricate organic nanocrystals, two common methods, reprecipitation and emulsion, are mainly used.[164,165] But both methods require relatively high energy input (*e.g.* vigorous mechanical stirring in batch processing) to achieve nano-range crystals[166] and often fail to meet all quality requirements of nanocrystals such as shape, structure, size distribution, *etc.*

Compared with conventional preparation methods of nanocrystals, microfluidic devices allow ultra-small material consumption, precise process control, superior mass and heat transfer performance, excellent reproducibility and monodispersity. Furthermore, in the microfluidic device, the mixing can be well controlled by adjusting the flow rates and various

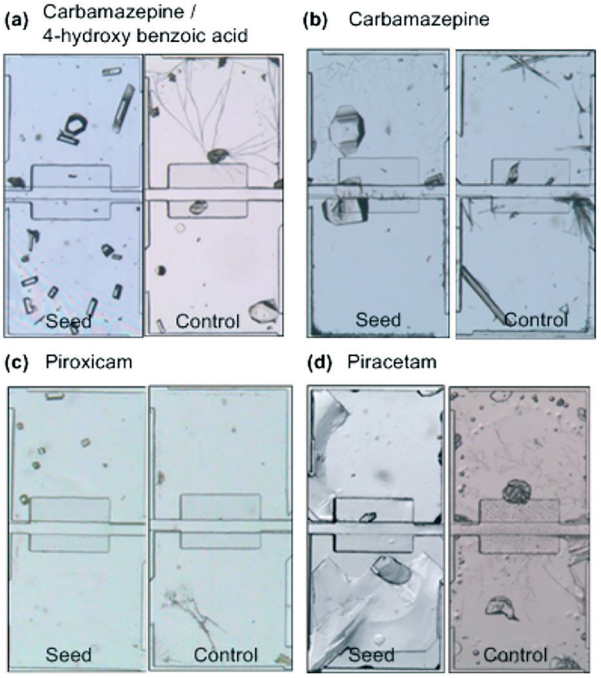

Fig. 9 Comparison of the final crystals with and without seeding (control). Reproduced from ref. 161 with permission from the American Chemical Society.

preparation conditions can be high-throughput screened by varying the operating parameters. In emulsion controlled nano-crystallizations, microfluidics can offer almost paralleled control over emulsion drop size and distribution variance.

Using microfluidic devices, nanocrystals with high quality and a narrow size distribution can be obtained because of the high reproducibility and precise control of operation parameters, such as time, temperature, droplet composition, *etc.*[119,167–169] Song *et al.* demonstrated that three different crystal structures of Co nanoparticles were synthesized by controlling the reaction time, flow rate and quenching procedure in a microfluidic device.[29] Sounart *et al.* synthesised cysteine-stabilized CdS bionanoparticles in a continuous-flow microreactor.[170] The microchannel used was 200 μm wide. Nanocrystal nucleation occurred at the centre of channels between two diffusion-limited laminar streams. The cysteine-stabilized CdS bioNP (CdS-Cys) photoluminescence intensity was observed under a CCD and an epifluorescence microscope, which was proportional to the nanoparticle concentration. Three-dimensional inorganic nanocrystal (NC) superlattices have been studied by Bodnarchuk *et al.*[171] Two driven approaches were explored to study the self-assembly of NCs. In destabilization-driven approaches, microfluidic plugs of different compositions were generated by varying the ratio of the solvent to the precipitant, then incubated to grow 3D superlattices. The NCs were monitored by optical microscopy. Another approach, evaporation-driven, relied on the microporous walls to evaporate the solvent slowly. Round-shaped NCs were observed by the evaporation-driven method while faceted crystals were observed by the destabilization-driven approach. NCs in the experiments were doped with Au, PbS, and CdSe, amongst others. They found that microfluidic plugs could also be used to grow 3D binary nanoparticle superlattices. Their latest study used droplet-based microfluidics for a real-time estimation of PbS nanoparticle size and concentration with a millisecond time resolution.[172] The methods succeeded in synthesizing PbS quantum dots, and implemented online measurements of colloidal crystallization at high temperature on rapid nucleation and growth stages. A two-stage mechanism was proposed to explain PbS nanoparticle formation: nucleation (formation of constant size nanoparticles continuously) and growth (consistent with the Ostwald ripening kinetic model).

Synthesis of organic nanocrystals by using microfluidic devices has recently received increasing attention.[72,173,174] In 2010, organic nanocrystals were synthesized in a 3D flow focusing microreactor by Génot *et al.*[173] The microreactor could control the supersaturation level and prevent crystals from fouling and clogging the channels. By changing the focusing ratio, large, unwanted crystals could be eliminated and rubrene nanocrystals with desired size were obtained. During the experiments, the flow rate of water/CTACI was fixed at 10 $\mu L\ min^{-1}$ while the flow rate of the solution varied from 0.5 to 3 $\mu L\ min^{-1}$. And the mixed-degree of water and rubrene solution was measured by confocal laser scanning microscopy. Later, the same microfluidic device was used to investigate the kinetics of organic nanocrystallization.[175] In this study, the side flow rate of an aqueous solution was between 10–50 $\mu L\ min^{-1}$, while the central flow of an organic solution was between 0.5–3 $\mu L\ min^{-1}$. Based on the variations of the relative flow rate, the focusing ratios changed accordingly. Eventually, nanoparticles with a controlled size were obtained.

Organic nanocrystals have also been investigated under microfluidic solution environments in confinement in mesoporous solids,[176] polymers or hydrogel matrices[177,178] or on self-assembled monolayers.[179] These methods have been successfully used to obtain organic nanocrystals. The end applications for solid confinement approaches are different in that, primary nanoparticles cannot be isolated and utilized, without dissolution of the substrate or applications where nanoparticles are dissolved. However, this does allow facile nanoparticle isolation, which is ordinarily very challenging. O'Mahoney *et al.* presented a method of simultaneous generation and stabilization of nano APIs compatible with a standard batch (and potentially continuous) pharmaceutical process equipment (ref). The use of confinement based micro fluid environments does present some specific limitations: limiting the direct observation *via* microscopy or spectroscopy (IR, Raman, NIR, *etc.*), broadening and masking XRD peaks, and difficulty in achieving the uniform distribution. Nanocrystals have also been prepared in larger bulk fluidic environments with polymers as stabilizer.[166] But this method suffers from poor control of particle size distributions, particle shape, severe scale-up issues, and large material requirements in development.

To summarize, microfluidics technology offers a new method for synthesizing nanocrystals. This technology can be

used to prepare nanocrystals with an ideal size, shape and structure. If combined with online analytical methods to monitor crystal nucleation and growth, it can also provide important fundamental data for understanding the mechanism of formation of nanocrystal preparation.

Determination of solubility and the metastable zone

As highlighted throughout this review, microfluidics is a high-throughput technology, which can simultaneously evaluate many separate experiments under different conditions simultaneously.[74,180] This is also highly beneficial in the ubiquitous solubility curve and metastable zone width measurements in crystallization development, which require measurement of the saturation concentration or dissolution point, at the full anticipated operating range of temperatures, pH values, concentrations, solvent & anti-solvent compositions, and counter-ion/co-former concentrations.[181] Laval *et al.* measured the solubility of adipic acid with less consumption of time, materials and experimental effort using microfluidics.[76] The microfluidic device had ten parallel and independent channels, and solution concentrations in adjacent channels had a gradual variation. A temperature gradient along the channels was created so that when the dissolution of crystals was observed in the droplets, the solubility could be estimated quickly and accurately. By this method, ten points of the solubility curve were determined simultaneously by using less than 250 μL of a solution. The concentration of the model compound in the droplets was monitored by using a confocal Raman microscope and was controlled to be stable in each channel before the outlet of the channel was sealed. Subsequently, Laval *et al.* used this approach to determine the potassium nitrate solubility curve and a new polymorph was observed for the first time during this study also.[182] The volume of a droplet stored in the microfluidic device was between 100–200 nL. And temperature was controlled by a Peltier module to form or dissolve a crystal in droplets. Crystals were investigated *in situ*, in-chip and in droplets by several analytical techniques, such as optical microscopy, confocal microscopy and Raman spectroscopy. It was found that two crystalline forms existed when the temperature was raised slowly. M. J. Anderson and his co-workers determined the solubility of glycerol kinase mutant gly230 under 64 different conditions while only consuming ~200 μg of the solute.[183] To determine the solubility, a unique mixture of different reagents and the protein solution was generated. 64 kinds of combinations between the precipitating agent and the protein were used to determine solubility through each phase diagram. The metastable zone width of lysozyme was determined in a microfluidic device by M. Ildefonso *et al.* in 2012.[104] The authors stored droplets (250 nL) of a solution with the same composition at different temperatures in four microfluidic devices. After 20 h, they observed and counted crystals which nucleated in each droplet. By using this method, accurate measurement of the metastable zone width with good reproducibility was achieved by performing only four experiments utilizing a large amount of droplets Around the same time, Dolega and coworkers determined the solubility diagrams of two model proteins automatically within hours.[184] To measure the supersolubility of a protein, droplets with different concentrations of the protein and the precipitant were formed and monitored. The application of electromagnetic valves and good design of the chip structure allowed droplets to mix rapidly and avoided contamination. Meanwhile, the volume of the droplets was precisely controlled. Workable microfluidic methods for measuring the solubility and metastable zone have been demonstrated. As would be anticipated, such approaches could provide significant benefits where large datasets are required and/or where the material is very expensive or has limited availability.

Protein crystallization with microfluidic devices

Predicting protein crystallization is a tricky problem since multiple factors influence the crystallization process of macromolecules.[185] Moreover, it is difficult to grow a protein crystal that is suitable for high-quality analysis because of the complexity of macromolecules. There are four basic protein crystallization methods: batch, dialysis, vapor diffusion, and liquid diffusion crystallization methods.[186] However, most traditional methods for investigating protein crystallization require considerable amounts of protein. Microfluidic devices offer advantages over conventional methods, such as low sample consumption, a non-convection environment, and high-throughput screening.[58] In microfluidic devices, it is easier to obtain large protein crystals with high quality for *in situ* analysis without physical damage.

Batch crystallization in microfluidic devices. One of the microfluidic systems used for batch crystallization is MPCS.[187] The CrystalCard contained two independent channels with 10 μL of useful volume with high-throughput crystallization, and each plug had a different concentration by varying the flow rates of solutions. Crystals were harvested by peeling the 100 μm bonding layer directly and then protected by liquid nitrogen for X-ray diffraction. Maeki *et al.* utilized a droplet-based microfluidic approach for protein crystallization.[188] The device was made up of a PDMS–Teflon capillary. The drop (2 nL) within a capillary was monitored by using a video camera. Besides, some crystals were moved to a glass capillary. To perform *in situ* X-ray diffraction, crystals should be fixed first. In this study, due to the high surface tension of a droplet, crystals could be fixed at the droplet interface without any manipulation. Diffraction data were directly collected from crystals in the capillary. Though the unfrozen crystal was damaged by the indirect action of X-ray, it was sufficient for analysis of the crystal structure. The influence of thickness and capillary materials on X-ray diffraction was also investigated and the results showed that no difference was observed.

Vapor diffusion crystallization in microfluidic devices. Yu and co-workers proposed a PDMS–glass microfluidic device for vapor diffusion crystallization, which allowed saturated

reagents to control the evaporation rates precisely and stably.[60] The gas and water permeability of PDMS supersaturated the protein solution by evaporating the solution. However, excessive evaporation caused large crystals to be broken. Therefore, the microfluidic device was immersed in paraffin oil to prevent further evaporation of the solution at the end of a trial. Wang *et al.*[59] presented a PDMS–glass microfluidic device. The device had 24 parallel units. The reaction chamber and precipitant channel were connected to the two sides of the vapor diffusion chamber by channels in each unit, allowing protein crystals to grow through the vapor diffusion process. Two-level capillary stop valves applied to the device guided 24 droplets into each unit and allowed vapor diffusion between the precipitant channel and the reaction chamber. Compared with conventional methods, the CD-like microfluidic chip was time-saving in mixing and dispensing for protein crystallization.

Liquid diffusion crystallization in microfluidic devices. Stojanoff *et al.* presented a microfluidic device for protein crystallization using liquid–liquid diffusion methods. In their method, protein and precipitant solutions were loaded into the channel from the opposite end, respectively.[115] When the solutions filled the channels, the device was sealed by removable film forms. Different mixing combinations generated an enormous number of conditions. In addition, the slow and controlled diffusion between solutions is favorable for the growth of high quality proteins. The device could be fixed at the goniometric head which was compatible with X-ray and allowed *in situ* X-ray diffraction. In 2014, Khvostichenko *et al.* demonstrated a 12-well array chip which will consume 60 nL of a protein solution per condition.[189] The chip consisted of four layers, including two layers of PDMS in the center, COC at the top and bottom. The mixing of different solutions through diffusion was controlled by valves. The capability of X-ray transparency enabled *in situ* X-ray diffraction.

Dialysis crystallization in microfluidic devices. Dialysis crystallization relies on water-permeable membranes to realize concentration and dilution of a protein solution.[186] It is difficult to perform dialysis crystallization in microfluidic devices because of the dimension limitation. The PhaseChip could store 1 nL of droplets in 100 wells and was demonstrated for protein nucleation and growth by dialysis.[107] Thousands of conditions could be screened with the consumption of 10 μg of a protein. The dialysis crystallization method has some advantages, such as reversible control of concentrations and reversible growth and dissolution of crystals. In the PhaseChip, water permeated through the dialysis from the reservoir to protein drops or the opposite. After the protein drops were loaded into the wells, dry air was introduced into the reservoir to concentrate drops, which promoted the emergence of a large number of small crystals or protein gel. Pure water was introduced into the reservoir to lower concentrations of the protein and salt. Finally, large and high-quality crystals were obtained while small crystals were dissolved.

Modern analytical technology for microfluidic crystallization

Modern analytical technologies, such as optical microscopy, crossed polarizers, X-ray diffraction, Raman spectroscopy, confocal Raman microscopy, scanning electron microscopy, have been used in the characterization of microfluidic crystallization.[145,182,190,191]

The most direct and intuitive observation method in microfluidic crystallization is optical microscopy. Images of crystals in the microfluidic devices can be captured by a stereo microscope equipped with a CCD camera.[182] Optical microscopy provides an approach to monitor crystal formation and morphology periodically by automated imaging acquisition and analysis.[111] In addition, scanning electron microscopy has also be used for studying crystal morphology.[146] However, optical microscopy cannot differentiate between the crystalline or amorphous state definitely. Due to birefringence of most crystals, crossed polarized filters can overcome the shortcoming for crystal identification.[192] In recent years, Raman microscopy has become a new trend in the study of crystallization. To obtain the Raman mapping images, the suitable Raman peak must be determined firstly. S. Nitahara's group found that the laser exposure time caused a significant difference in Raman intensities between a crystal and a solution.[191] The Raman mapping also has the potential to identify the position of a crystal in droplets. Depending on the change of Raman intensities with time, confocal Raman microscopy can be used to determine crystal growth in droplets under any cumbersome operations.[193] And time evolution of Raman mapping images can also show the change of concentration during crystal nucleation and growth.[191]

In situ Raman spectra and X-ray diffraction patterns can be effectively used to verify the form and structure of crystals in the microfluidic devices. To achieve this, the microfluidic devices should be transparent to Raman spectra or X-rays.[111,194,195] In terms of powder X-ray diffraction, it can be used to determine the structure of crystals that are small or fragile. When conducting a single crystal X-ray experiment which is more accurate than powder X-ray diffraction, the size of microfluidic devices should be appropriately designed to host large crystals.[161,189] Although X-ray diffraction can evaluate the quality of crystals,[106] sometimes, high-flux X-ray beams may cause radiation damage to the crystals in the liquid-phase.[196,197] In that case, cryoprotection becomes vital to reduce radiation damage.[198] M. Maeki *et al.* have demonstrated that the quality of crystals without cryoprotection decreased dramatically with the increase in the measurement time.[63,190] The results also indicated that the crystals under cryoprotection did not deteriorate. On the other hand, cryoprotection also has limitations because of solvent conditions and volume change. For crystals that are resistant to X-ray radiation damage, X-ray diffraction data for determining the crystal structure should be collected at room temperature.[189,194,199] F. Pinker and his co-workers have confirmed

that the crystal structure obtained by X-ray diffraction at room temperature is reliable using automated synchrotron beamlines.[194] To minimize radiation damage, the authors adjusted the exposure time and oscillation range. Another advantage of room temperature diffraction is that it can eliminate the tedious step of cryoprotection. E. M. Horstman' group collected on-chip X-ray data of different crystals at room temperature and then they determined the structure by merging X-ray data of multiple crystals (Fig. 10).[161]

In recent years, as a simple and efficient method to identify crystal forms, the on-chip Raman method has attracted more and more attention.[200] On-chip Raman spectroscopy can be used to provide stoichiometric information and determine polymorphs, co-crystals, and pharmaceutical salts.[111,146] M. R. Thorson *et al.* identified four different naproxen salts and five different ephedrine salts using Raman spectroscopy.[192] On-chip Raman spectroscopy helps to realize the screening of crystal forms in the early stage of drug manufacture with fewer amounts of materials. S. Goyal *et al.* confirmed crystalline solid forms of PCs by Raman spectroscopy and compared the on-chip Raman data with off-chip Raman data of nine caffeine co-crystals (shown in Fig. 11).[111] Later, they described a microfluidic platform that could be used to screen co-crystals and polymorphs by an on-chip Raman method in solvent evaporation and anti-solvent crystallization, respectively.[160] The obtained Raman spectra of crystal forms using on-chip Raman analysis were found to be consistent with the results obtained by off-chip analysis.

Conclusions

Application of microfluidic devices for investigating crystallization is attracting more and more attention due to the special miniaturized environments of microfluidic devices. Compared to the conventional crystallization methods, the microfluidic method turns out to be a high-throughput, fast and reliable method for investigating crystallization processes. This review summarized and analysed the state of art applications of microfluidics in the crystallization arena, including crystal nucleation and crystal growth, polymorph and co-crystal screening, nanocrystals preparation, solubility and metastable zone determination. The materials and structures of microfluidic devices for crystallization processes and the modern analytical methods for microfluidic crystallization were also summarized and analysed.

Many researchers have demonstrated that crystals with an ideal shape, size and crystal structure could be obtained by microfluidic technology. Arrays of conditions conducted in one experiment could provide possibility for nucleation estimation, crystal form screening, and phase diagram plotting. And these targets could be more accurately achieved in less time and by consuming a small amount of materials. On-chip characterization could avoid the damage caused by the downstream treatment in traditional experiments.

Indeed, great breakthroughs have been made in the applications of microfluidic devices in the crystallization arena. However, there are still some challenges in practical applications of microfluidic devices for crystallization. For example, blockage of the channels is an issue for crystallization in microfluidic devices since the crystals are prone to stick to the wall of the channels. To overcome this problem, better design of the channel structure and better materials need to be proposed. Theoretically, the current nucleation model can predict empty droplets in experiments, but fail to predict the exact number of crystals in droplets.[109] A more accurate model needs to be built up to predict the exact number of crystals in droplets. In addition, better temperature control technologies for microfluidic devices are required for screening wider range of supersaturation. In terms of *in situ*

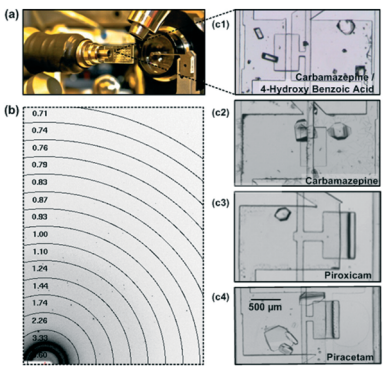

Fig. 10 (a) Microfluidic device mounted on an XRD. (b) Diffraction data of crystal products. (c) Different crystals of different compounds in a microfluidic device. Reproduced from ref. 161 with permission from the American Chemical Society.

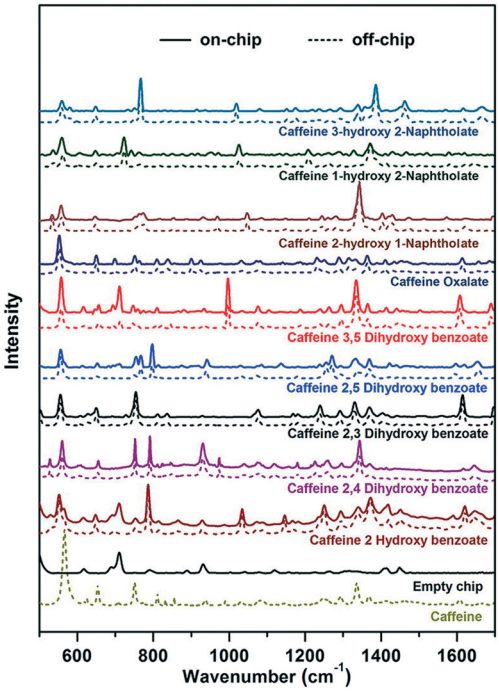

Fig. 11 Raman spectroscopy data of nine caffeine co-crystals on-chip and off-chip. Reproduced from ref. 111 with permission from the American Chemical Society.

characterization methods, although hybrid PDMS–COC is transparent to X-ray diffraction or Raman spectroscopy, it has compatibility problems with most of organic solvents. Hence, new modification methods for the fabrication of microfluidic devices need to be developed. If all these issues could be addressed, microfluidic devices will be more widely used in crystallization and will definitely promote the development of the crystallization theory and technology.

Acknowledgements

This research is financially supported by the National Natural Science Foundation of China (No. 21376165) and the National Key Research and Development Program of China (No. 2016YFB0600504.)

Notes and references

1 H. Seki and Y. Su, *Chem. Eng. Sci.*, 2015, **133**, 16–23.
2 M. O. Besenhard, P. Neugebauer, C.-D. Ho and J. G. Khinast, *Cryst. Growth Des.*, 2015, **15**, 1683–1691.
3 M. Barrett, M. McNamara, H. Hao, P. Barrett and B. Glennon, *Chem. Eng. Res. Des.*, 2010, **88**, 1108–1119.
4 K. Adrjanowicz, A. Grzybowski, K. Grzybowska, J. Pionteck and M. Paluch, *Cryst. Growth Des.*, 2013, **13**, 4648–4654.
5 H. S. Lee, *J. Chem. Phys.*, 2013, **139**, 104909.
6 H. Akiba, M. Ichiji, H. Nagao and I. Hirasawa, *Chem. Eng. Technol.*, 2015, **38**, 1068–1072.
7 A. Erriguible, T. Fadli and P. Subra-Paternault, *Comput. Chem. Eng.*, 2013, **52**, 1–9.
8 Z. Wu, G. Zhong, Z. Zhang, X. Zhou, Z. Wang and X. Huang, *J. Cryst. Growth*, 2015, **426**, 110–116.
9 Y. Jia and X.-Y. Liu, *J. Phys. Chem. B*, 2006, **110**, 6949–6955.
10 A. Lewis and M. Mangere, *Chem. Eng. Technol.*, 2011, **34**, 517–524.
11 S. Teychené and B. Biscans, *Cryst. Growth Des.*, 2008, **8**, 1133–1139.
12 C. Sauter, K. Dhouib and B. Lorber, *Cryst. Growth Des.*, 2007, **7**, 2247–2250.
13 C. L. Hansen, E. Skordalakes, J. M. Berger and S. R. Quake, *Proc. Natl. Acad. Sci. U. S. A.*, 2002, **99**, 16531–16536.
14 B. Zheng, L. S. Roach and R. F. Ismagilov, *J. Am. Chem. Soc.*, 2003, **125**, 11170–11171.
15 C. W. Carruthers Jr., C. Gerdts, M. D. Johnson and P. Webb, *PLoS One*, 2013, **8**, e82298.
16 S. Vyawahare, A. D. Griffiths and C. A. Merten, *Chem. Biol.*, 2010, **17**, 1052–1065.
17 A. Feuerborn, A. Prastowo, P. R. Cook and E. Walsh, *Lab Chip*, 2015, **15**, 3766–3775.
18 C. L. Hansen, S. Classen, J. M. Berger and S. R. Quake, *J. Am. Chem. Soc.*, 2006, **128**, 3142–3143.
19 C. Henrist, J. P. Mathieu, C. Vogels, A. Rulmont and R. Cloots, *J. Cryst. Growth*, 2003, **249**, 321–330.
20 J. Leng, B. Lonetti, P. Tabeling, M. Joanicot and A. Ajdari, *Phys. Rev. Lett.*, 2006, **96**, 084503.
21 J.-U. Shim, G. Cristobal, D. R. Link, T. Thorsen, Y. Jia, K. Piattelli and S. Fraden, *J. Am. Chem. Soc.*, 2007, **129**, 8825–8835.
22 Z. T. Cygan, J. T. Cabral, K. L. Beers and E. J. Amis, *Langmuir*, 2005, **21**, 3629–3634.
23 M. J. Jebrail and A. R. Wheeler, *Curr. Opin. Chem. Biol.*, 2010, **14**, 574–581.
24 L. Li and R. F. Ismagilov, *Annu. Rev. Biophys.*, 2010, **39**, 139–158.
25 N. Hao, J. Y. Li, M. Xiong, X. H. Xia, J. J. Xu and H. Y. Chen, *ACS Appl. Mater. Interfaces*, 2014, **6**, 11869–11873.
26 M. R. Thorson, S. Goyal, B. R. Schudel, C. F. Zukoski, G. G. Zhang, Y. Gong and P. J. Kenis, *Lab Chip*, 2011, **11**, 3829–3837.
27 S. Dev, K. S. Iyer and C. L. Raston, *Lab Chip*, 2011, **11**, 3214–3217.
28 L. Frenz, A. El Harrak, M. Pauly, S. Begin-Colin, A. D. Griffiths and J. C. Baret, *Angew. Chem., Int. Ed.*, 2008, **47**, 6817–6820.
29 Y. Song, H. Modrow, L. L. Henry, C. K. Saw, E. E. Doomes, V. Palshin, J. Hormes and C. S. S. R. Kumar, *Chem. Mater.*, 2006, **18**, 2817–2827.
30 K. Ren, J. Zhou and H. Wu, *Acc. Chem. Res.*, 2013, **46**, 2396–2406.
31 L. Che-Hsin, L. Gwo-Bin, L. Yen-Heng and C. Guan-Liang, *J. Micromech. Microeng.*, 2001, **11**, 726.
32 A. Berthold, L. Nicola, P. Sarro and M. Vellekoop, *Sens. Actuators, A*, 2000, **82**, 224–228.
33 C. Qiang, L. Gang, J. Qing-Hui, Z. Jian-Long, R. Qiu-Shi and X. Yuan-Sen, *J. Microelectromech. Syst.*, 2007, **16**, 1193–1200.
34 A. I. Toldy, A. Z. M. Badruddoza, L. Zheng, T. A. Hatton, R. Gunawan, R. Rajagopalan and S. A. Khan, *Cryst. Growth Des.*, 2012, **12**, 3977–3982.
35 E. Q. Li, J. M. Zhang and S. T. Thoroddsen, *J. Micromech. Microeng.*, 2013, **24**, 015019.
36 M. Pollack, A. Shenderov and R. Fair, *Lab Chip*, 2002, **2**, 96–101.
37 A. Sanjoh and T. Tsukihara, *J. Cryst. Growth*, 1999, **196**, 691–702.
38 H. Chen, X. Li, L. Wang and P. C. H. Li, *Talanta*, 2010, **81**, 1203–1208.
39 X. Fang, Y. Liu, J. Kong and X. Jiang, *Anal. Chem.*, 2010, **82**, 3002–3006.
40 C. Longuet, A. Yamada, Y. Chen, D. Baigl and J. Fattaccioli, *J. Cryst. Growth*, 2014, **386**, 179–182.
41 G. Li and S. Xu, *Mater. Des.*, 2015, **81**, 82–86.
42 J. N. Lee, C. Park and G. M. Whitesides, *Anal. Chem.*, 2003, **75**, 6544–6554.
43 J. C. McDonald and G. M. Whitesides, *Acc. Chem. Res.*, 2002, **35**, 491–499.
44 A. R. Abate, D. Lee, T. Do, C. Holtze and D. A. Weitz, *Lab Chip*, 2008, **8**, 516–518.
45 M. Domenichini, R. Sahai, P. Castrataro, R. Valsecchi, C. Tonelli, F. Greco and P. Dario, *Microfluid. Nanofluid.*, 2013, **15**, 753–762.

46 C.-W. Tsao and D. L. DeVoe, *Microfluid. Nanofluid.*, 2008, **6**, 1–16.
47 A. Muck, J. Wang, M. Jacobs, G. Chen, M. P. Chatrathi, V. Jurka, Z. Výborný, S. D. Spillman, G. Sridharan and M. J. Schöning, *Anal. Chem.*, 2004, **76**, 2290–2297.
48 S. Mukhopadhyay, J. P. Banerjee, A. Mathur, M. Tweedie, J. A. McLaughlin and S. S. Roy, *Surf. Rev. Lett.*, 2015, **22**, 1550050.
49 A. Shamsi, A. Amiri, P. Heydari, H. Hajghasem, M. Mohtashamifar and M. Esfandiari, *Microsystem Technologies*, 2013, **20**, 1925–1931.
50 A. Toossi, H. Moghadas, M. Daneshmand and D. Sameoto, *J. Micromech. Microeng.*, 2015, **25**, 085008.
51 B. Subramanian, N. Kim, W. Lee, D. A. Spivak, D. E. Nikitopoulos, R. L. McCarley and S. A. Soper, *Langmuir*, 2011, **27**, 7949–7957.
52 M. Madou, *Fundamentals of Microfabrication*, CRC Press, New York, 1997, pp. 193–199.
53 S. A. Soper, S. M. Ford, S. Qi, R. L. McCarley, K. Kelly and M. C. Murphy, *Anal. Chem.*, 2000, **72**, 642A–651A.
54 N. Maluf and K. Williams, *Introduction to microelectromechanical systems engineering*, Artech House, 2004.
55 L. Martynova, L. E. Locascio, M. Gaitan, G. W. Kramer, R. G. Christensen and W. A. MacCrehan, *Anal. Chem.*, 1997, **69**, 4783–4789.
56 B.-H. Jo, L. M. Van Lerberghe, K. M. Motsegood and D. J. Beebe, *J. Microelectromech. Syst.*, 2000, **9**, 76–81.
57 J. R. Anderson, D. T. Chiu, H. Wu, O. Schueller and G. M. Whitesides, *Electrophoresis*, 2000, **21**, 27–40.
58 G. Li, Q. Chen, J. Li, X. Hu and J. Zhao, *Anal. Chem.*, 2010, **82**, 4362–4369.
59 L. Wang, K. Sun, X. Hu, G. Li, Q. Jin and J. Zhao, *Sens. Actuators, B*, 2015, **219**, 105–111.
60 Y. Yu, X. Wang, D. Oberthür, A. Meyer, M. Perbandt, L. Duan and Q. Kang, *J. Appl. Crystallogr.*, 2011, **45**, 53–60.
61 P. Laval, J.-B. Salmon and M. Joanicot, *J. Cryst. Growth*, 2007, **303**, 622–628.
62 C. Wang, D. K. Ye, Y. Y. Wang, T. Lu and X. H. Xia, *Lab Chip*, 2013, **13**, 1546–1553.
63 M. Maeki, A. S. Pawate, K. Yamashita, M. Kawamoto, M. Tokeshi, P. J. A. Kenis and M. Miyazaki, *Anal. Chem.*, 2015, **87**, 4194–4200.
64 E. Quevedo, J. Steinbacher and D. T. McQuade, *J. Am. Chem. Soc.*, 2005, **127**, 10498–10499.
65 H. Peng, Z. Xu, S. Chen, Z. Zhang, B. Li and L. Ge, *Colloids Surf., A*, 2015, **468**, 271–279.
66 M. Ildefonso, N. Candoni and S. Veesler, *Org. Process Res. Dev.*, 2012, **16**, 556–560.
67 R. D. Dombrowski, J. D. Litster, N. J. Wagner and Y. He, *Chem. Eng. Sci.*, 2007, **62**, 4802–4810.
68 S. Zhang, N. Ferté, N. Candoni and S. Veesler, *Org. Process Res. Dev.*, 2015, **19**, 1837–1841.
69 J. Puigmarti-Luis, *Chem. Soc. Rev.*, 2014, **43**, 2253–2271.
70 M. Sultana and K. F. Jensen, *Cryst. Growth Des.*, 2012, **12**, 6260–6266.
71 Y. F. Su, H. Kim, S. Kovenklioglu and W. Y. Lee, *J. Solid State Chem.*, 2007, **180**, 2625–2629.
72 K. Jasch, N. Barth, S. Fehr, H. Bunjes, W. Augustin and S. Scholl, *Chem. Eng. Technol.*, 2009, **32**, 1806–1814.
73 P. Moschou, M. H. J. M. de Croon, J. van der Schaaf and J. C. Schouten, *Rev. Chem. Eng.*, 2014, **30**, 127–138.
74 W. C. Chao, J. Collins, S. W. Wang, G. Li, M. Bachman and A. P. Lee, *Conf. Proc. IEEE Eng. Med. Biol. Soc.*, 2004, **4**, 2623–2626.
75 P. Laval, A. Crombez and J.-B. Salmon, *Langmuir*, 2009, **25**, 1836–1841.
76 P. Laval, N. Lisai, J. B. Salmon and M. Joanicot, *Lab Chip*, 2007, **7**, 829–834.
77 W.-N. Wang, A. Purwanto, I. W. Lenggoro, K. Okuyama, H. Chang and H. D. Jang, *Ind. Eng. Chem. Res.*, 2008, **47**, 1650–1659.
78 Š. Selimović, Y. Jia and S. Fraden, *Cryst. Growth Des.*, 2009, **9**, 1806–1810.
79 X. Casadevall i Solvas and A. de Mello, *Chem. Commun.*, 2011, **47**, 1936–1942.
80 Y. Pang, J. Liu, H. Li and J. Lin, *Sci. China, Ser. B: Chem.*, 2009, **52**, 1014–1020.
81 S. Y. Teh, R. Lin, L. H. Hung and A. P. Lee, *Lab Chip*, 2008, **8**, 198–220.
82 S. L. Perry, G. W. Roberts, J. D. Tice, R. B. Gennis and P. J. A. Kenis, *Cryst. Growth Des.*, 2009, **9**, 2566–2569.
83 B. T. Lau, C. A. Baitz, X. P. Dong and C. L. Hansen, *J. Am. Chem. Soc.*, 2007, **129**, 454–455.
84 M. J. Jebrail and A. R. Wheeler, *Anal. Chem.*, 2008, **81**, 330–335.
85 L. Malic, D. Brassard, T. Veres and M. Tabrizian, *Lab Chip*, 2010, **10**, 418–431.
86 K. Choi, A. H. Ng, R. Fobel and A. R. Wheeler, *Annu. Rev. Anal. Chem.*, 2012, **5**, 413–440.
87 S. K. Cho, H. Moon and C.-J. Kim, *J. Microelectromech. Syst.*, 2003, **12**, 70–80.
88 W. C. Nelson and C. J. C. Kim, *J. Adhes. Sci. Technol.*, 2012, **26**, 1747–1771.
89 N. Mei, B. Seale, A. H. Ng, A. R. Wheeler and R. Oleschuk, *Anal. Chem.*, 2014, **86**, 8466–8472.
90 A. R. Wheeler, H. Moon, C. A. Bird, R. R. Ogorzalek Loo, C.-J. C. Kim, J. A. Loo and R. L. Garrell, *Anal. Chem.*, 2005, **77**, 534–540.
91 M. J. Jebrail, V. N. Luk, S. C. Shih, R. Fobel, A. H. Ng, H. Yang, S. L. Freire and A. R. Wheeler, *J. Visualized Exp.*, 2009, e1603.
92 J. Hong, Y. K. Kim, D. J. Won, J. Kim and S. J. Lee, *Sci. Rep.*, 2015, **5**, 10685.
93 S. J. Lee, S. Lee and K. H. Kang, *J. Visualization*, 2011, **14**, 259–264.
94 S. J. Lee, S. Lee and K. H. Kang, *Appl. Phys. Lett.*, 2012, **100**, 081604.
95 F. Lapierre, Y. Coffinier, R. Boukherroub and V. Thomy, *Langmuir*, 2013, **29**, 13346–13351.
96 H. Ren, R. B. Fair, M. G. Pollack and E. J. Shaughnessy, *Sens. Actuators, B*, 2002, **87**, 201–206.
97 W. C. Nelson, I. Peng, G.-A. Lee, J. A. Loo, R. L. Garrell and C.-J. Kim, *Anal. Chem.*, 2010, **82**, 9932–9937.

98 T. Kokalj, E. Pérez-Ruiz and J. Lammertyn, *New Biotechnol.*, 2015, **32**, 485–503.
99 W.-B. Du, M. Sun, S.-Q. Gu, Y. Zhu and Q. Fang, *Anal. Chem.*, 2010, **82**, 9941–9947.
100 F. Y. Ushikubo, F. S. Birribilli, D. R. B. Oliveira and R. L. Cunha, *Microfluid. Nanofluid.*, 2014, **17**, 711–720.
101 R. A. L. Leon, W. Y. Wan, A. Z. M. Badruddoza, T. A. Hatton and S. A. Khan, *Cryst. Growth Des.*, 2014, **14**, 140–146.
102 B. Riechers, F. Wittbracht, A. Hutten and T. Koop, *Phys. Chem. Chem. Phys.*, 2013, **15**, 5873–5887.
103 S. Teychené and B. Biscans, *Chem. Eng. Sci.*, 2012, **77**, 242–248.
104 M. Ildefonso, E. Revalor, P. Punniam, J. Salmon, N. Candoni and S. Veesler, *J. Cryst. Growth*, 2012, **342**, 9–12.
105 P. Laval, N. Lisai, J.-B. Salmon and M. Joanicot, *Lab Chip*, 2007, **7**, 829–834.
106 B. Zheng, J. D. Tice, L. S. Roach and R. F. Ismagilov, *Angew. Chem., Int. Ed.*, 2004, **43**, 2508–2511.
107 J.-U. Shim, G. Cristobal, D. R. Link, T. Thorsen and S. Fraden, *Cryst. Growth Des.*, 2007, **7**, 2192–2194.
108 Y. Vitry, S. Teychené, S. Charton, F. Lamadie and B. Biscans, *Chem. Eng. Sci.*, 2015, **133**, 54–61.
109 V. Bhamidi, S. H. Lee, G. He, P. S. Chow, R. B. H. Tan, C. F. Zukoski and P. J. A. Kenis, *Cryst. Growth Des.*, 2015, **15**, 3299–3306.
110 M. R. Thorson, S. Goyal, Y. Gong, G. G. Z. Zhang and P. J. A. Kenis, *CrystEngComm*, 2012, **14**, 2404.
111 S. Goyal, M. R. Thorson, G. G. Z. Zhang, Y. Gong and P. J. A. Kenis, *Cryst. Growth Des.*, 2012, **12**, 6023–6034.
112 B. G. Abdallah, C. Kupitz, P. Fromme and A. Ros, *ACS Nano*, 2013, **7**, 10534–10543.
113 B. R. Takulapalli, J. Qiu, D. M. Magee, P. Kahn, A. Brunner, K. Barker, S. Means, S. Miersch, X. Bian, A. Mendoza, F. Festa, K. Syal, J. G. Park, J. LaBaer and P. Wiktor, *J. Proteome Res.*, 2012, **11**, 4382–4391.
114 B. G. Abdallah, S. Roy-Chowdhury, R. Fromme, P. Fromme and A. Ros, *Cryst. Growth Des.*, 2016, **16**, 2074–2082.
115 V. Stojanoff, J. Jakoncic, D. A. Oren, V. Nagarajan, J. C. Poulsen, M. A. Adams-Cioaba, T. Bergfors and M. O. Sommer, *Acta Crystallogr., Sect. F: Struct. Biol. Cryst. Commun.*, 2011, **67**, 971–975.
116 L. Li, W. Du and R. F. Ismagilov, *J. Am. Chem. Soc.*, 2010, **132**, 112–119.
117 M. Lounaci, Y. Chen and P. Rigolet, *Microelectron. Eng.*, 2010, **87**, 750–752.
118 Y. Zhu, L. N. Zhu, R. Guo, H. J. Cui, S. Ye and Q. Fang, *Sci Rep.*, 2014, **4**, 5046.
119 S. Zhang, N. Ferté, N. Candoni and S. Veesler, *Org. Process Res. Dev.*, 2015, **19**, 1837–1841.
120 Y. Pan, J. Yao, L. Zhang and N. Xu, *Ind. Eng. Chem. Res.*, 2009, **48**, 8471–8477.
121 E. M. Chan, R. A. Mathies and A. P. Alivisatos, *Nano Lett.*, 2003, **3**, 199–201.
122 H. Wang, A. Tashiro, H. Nakamura, M. Uehara, M. Miyazaki, T. Watari and H. Maeda, *J. Mater. Res.*, 2004, **19**, 3157–3161.
123 S. V. Akella, A. Mowitz, M. Heymann and S. Fraden, *Cryst. Growth Des.*, 2014, **14**, 4487–4509.
124 K. Ando, A.-Q. Liu and C.-D. Ohl, *Phys. Rev. Lett.*, 2012, **109**, 044501.
125 C. A. Stan, G. F. Schneider, S. S. Shevkoplyas, M. Hashimoto, M. Ibanescu, B. J. Wiley and G. M. Whitesides, *Lab Chip*, 2009, **9**, 2293–2305.
126 K. Chen, L. Goh, G. He, P. J. A. Kenis, C. F. Zukoski and R. D. Braatz, *Chem. Eng. Sci.*, 2012, **77**, 235–241.
127 L. Goh, K. Chen, V. Bhamidi, G. He, N. C. Kee, P. J. Kenis, C. F. Zukoski 3rd and R. D. Braatz, *Cryst. Growth Des.*, 2010, **10**, 2515–2521.
128 M. Ildefonso, N. Candoni and S. Veesler, *Cryst. Growth Des.*, 2011, **11**, 1527–1530.
129 T. A. Prileszky and E. M. Furst, *Langmuir*, 2016, **32**, 5141–5146.
130 M. Ildefonso, N. Candoni and S. Veesler, *Cryst. Growth Des.*, 2013, **13**, 2107–2110.
131 D. Rossi, A. Gavriilidis, S. Kuhn, M. A. Candel, A. G. Jones, C. Price and L. Mazzei, *Cryst. Growth Des.*, 2015, **15**, 1784–1791.
132 J. Lu, J. D. Litster and Z. K. Nagy, *Cryst. Growth Des.*, 2015, **15**, 3645–3651.
133 S. Xu, Z. Nie, M. Seo, P. Lewis, E. Kumacheva, H. A. Stone, P. Garstecki, D. B. Weibel, I. Gitlin and G. M. Whitesides, *Angew. Chem.*, 2005, **117**, 734–738.
134 R. D. Dombrowski, J. D. Litster, N. J. Wagner and Y. He, *AIChE J.*, 2010, **56**, 79–91.
135 P. H. Hoang, H. Park and D.-P. Kim, *J. Am. Chem. Soc.*, 2011, **133**, 14765–14770.
136 V. Sebastian Cabeza, S. Kuhn, A. A. Kulkarni and K. F. Jensen, *Langmuir*, 2012, **28**, 7007–7013.
137 J. Kim and S. A. Vanapalli, *Langmuir*, 2013, **29**, 12307–12316.
138 A. I. Toldy, L. Zheng, A. Z. M. Badruddoza, T. A. Hatton and S. A. Khan, *Cryst. Growth Des.*, 2014, **14**, 3485–3492.
139 R. Hiremath, J. A. Basile, S. W. Varney and J. A. Swift, *J. Am. Chem. Soc.*, 2005, **127**, 18321–18327.
140 F. Quist and A. Kakkar, *J. Colloid Interface Sci.*, 2007, **313**, 378–382.
141 J. Vollmeyer, F. Eberhagen, S. Hoger and S. S. Jester, *Beilstein J. Org. Chem.*, 2014, **10**, 2774–2782.
142 X. Hou, Y. Feng, P. Zhang, H. Wei and L. Dang, *Cryst. Growth Des.*, 2015, **15**, 4918–4924.
143 N. Sánchez-Pastor, A. M. Gigler, J. A. Cruz, S.-H. Park, G. Jordan and L. Fernández-Díaz, *Cryst. Growth Des.*, 2011, **11**, 3081–3089.
144 H. B. Eral, M. O'Mahony, R. Shaw, B. L. Trout, A. S. Myerson and P. S. Doyle, *Chem. Mater.*, 2014, **26**, 6213–6220.
145 M. L. Peterson, S. L. Morissette, C. McNulty, A. Goldsweig, P. Shaw, M. LeQuesne, J. Monagle, N. Encina, J. Marchionna and A. Johnson, *J. Am. Chem. Soc.*, 2002, **124**, 10958–10959.

146 B. Ji, M. Cusack, A. Freer, P. S. Dobson, N. Gadegaard and H. Yin, *Integr. Biol.*, 2010, **2**, 528–535.
147 L. Geneviciute, N. Florio and S. Lee, *Cryst. Growth Des.*, 2011, **11**, 4440–4448.
148 J.-P. Astier and S. Veesler, *Cryst. Growth Des.*, 2008, **8**, 4215–4219.
149 C. B. Aakeroy and D. J. Salmon, *CrystEngComm*, 2005, **7**(72), 439–448.
150 S. Aitipamula, V. R. Vangala, P. S. Chow and R. B. H. Tan, *Cryst. Growth Des.*, 2012, **12**, 5858–5863.
151 N. Chieng, M. Hubert, D. Saville, T. Rades and J. Aaltonen, *Cryst. Growth Des.*, 2009, **9**, 2377–2386.
152 D. J. Good and N. R. Rodríguez-Hornedo, *Cryst. Growth Des.*, 2009, **9**, 2252–2264.
153 M. K. Stanton and A. Bak, *Cryst. Growth Des.*, 2008, **8**, 3856–3862.
154 B. Xue, M. Mao, Y. Liu, J. Guo, J. Li and E. Liu, *J. Cryst. Growth*, 2016, **442**, 110–113.
155 L. Padrela, M. A. Rodrigues, S. P. Velaga, A. C. Fernandes, H. A. Matos and E. G. de Azevedo, *J. Supercrit. Fluids*, 2010, **53**, 156–164.
156 A. Lemmerer, D. A. Adsmond, C. Esterhuysen and J. Bernstein, *Cryst. Growth Des.*, 2013, **13**, 3935–3952.
157 X. Shi, S. Y. Wong, X. Yang and A. S. Myerson, *CrystEngComm*, 2013, **15**, 7450.
158 M. Mukaida, Y. Watanabe, K. Sugano and K. Terada, *Eur. J. Pharm. Sci.*, 2015, **79**, 61–66.
159 S. Goyal, M. R. Thorson, C. L. Schneider, G. G. Zhang, Y. Gong and P. J. Kenis, *Lab Chip*, 2013, **13**, 1708–1723.
160 S. Goyal, A. E. Economou, T. Papadopoulos, E. M. Horstman, G. G. Z. Zhang, Y. Gong and P. J. A. Kenis, *RSC Adv.*, 2016, **6**, 13286–13296.
161 E. M. Horstman, S. Goyal, A. Pawate, G. Lee, G. G. Zhang, Y. Gong and P. J. Kenis, *Cryst. Growth Des.*, 2015, **15**, 1201–1209.
162 W. Lu and C. M. Lieber, *Nat. Mater.*, 2007, **6**, 841–850.
163 S. E. Gratton, S. S. Williams, M. E. Napier, P. D. Pohlhaus, Z. Zhou, K. B. Wiles, B. W. Maynor, C. Shen, T. Olafsen and E. T. Samulski, *Acc. Chem. Res.*, 2008, **41**, 1685–1695.
164 R. O. Al-Kaysi, A. M. Müller, T.-S. Ahn, S. Lee and C. J. Bardeen, *Langmuir*, 2005, **21**, 7990–7994.
165 E. Kwon, H. Oikawa, H. Kasai and H. Nakanishi, *Cryst. Growth Des.*, 2007, **7**, 600–602.
166 K. Ujiiye-Ishii, E. Kwon, H. Kasai, H. Nakanishi and H. Oikawa, *Cryst. Growth Des.*, 2008, **8**, 369–371.
167 H. Nakamura, Y. Yamaguchi, M. Miyazaki, H. Maeda, M. Uehara and P. Mulvaney, *Chem. Commun.*, 2002, 2844–2845.
168 H. Nakamura, A. Tashiro, Y. Yamaguchi, M. Miyazaki, T. Watari, H. Shimizu and H. Maeda, *Lab Chip*, 2004, **4**, 237–240.
169 J. D. Winterton, D. R. Myers, J. M. Lippmann, A. P. Pisano and F. M. Doyle, *J. Nanopart. Res.*, 2008, **10**, 893–905.
170 T. Sounart, P. Safier, J. Voigt, J. Hoyt, D. Tallant, C. Matzke and T. Michalske, *Lab Chip*, 2007, **7**, 908–915.
171 M. I. Bodnarchuk, L. Li, A. Fok, S. Nachtergaele, R. F. Ismagilov and D. V. Talapin, *J. Am. Chem. Soc.*, 2011, **133**, 8956–8960.
172 I. Lignos, S. Stavrakis, A. Kilaj and A. J. de Mello, *Small*, 2015, **11**, 4009–4017.
173 V. Génot, S. Desportes, C. Croushore, J.-P. Lefèvre, R. B. Pansu, J. A. Delaire and P. R. von Rohr, *Chem. Eng. J.*, 2010, **161**, 234–239.
174 L. Capretto, D. Carugo, S. Mazzitelli, C. Nastruzzi and X. Zhang, *Adv. Drug Delivery Rev.*, 2013, **65**, 1496–1532.
175 Y. Liao, V. Génot, J.-F. Audibert and R. B. Pansu, *Microfluid. Nanofluid.*, 2016, **20**, 1–11.
176 K. K. Qian and R. H. Bogner, *J. Pharm. Sci.*, 2012, **101**, 444–463.
177 X. Yang, T.-C. Ong, V. K. Michaelis, S. Heng, R. G. Griffin and A. S. Myerson, *CrystEngComm*, 2015, **17**, 6044–6052.
178 H. Wang, B. A. Holmberg and Y. Yan, *J. Am. Chem. Soc.*, 2003, **125**, 9928–9929.
179 S. Rosenne, E. Grinvald, E. Shirman, L. Neeman, S. Dutta, O. Bar-Elli, R. Ben-Zvi, E. Oksenberg, P. Milko and V. Kalchenko, *Nano Lett.*, 2015, **15**, 7232–7237.
180 P. G. Vekilov and O. Galkin, *Colloids Surf., A*, 2003, **215**, 125–130.
181 C. L. Hansen, M. O. Sommer and S. R. Quake, *Proc. Natl. Acad. Sci. U. S. A.*, 2004, **101**, 14431–14436.
182 P. Laval, C. Giroux, J. Leng and J.-B. Salmon, *J. Cryst. Growth*, 2008, **310**, 3121–3124.
183 M. J. Anderson, B. DeLaBarre, A. Raghunathan, B. O. Palsson, A. T. Brunger and S. R. Quake, *Biochemistry*, 2007, **46**, 5722–5731.
184 M. E. Dolega, S. Jakiela, M. Razew, A. Rakszewska, O. Cybulski and P. Garstecki, *Lab Chip*, 2012, **12**, 4022–4025.
185 A. McPherson, *Methods*, 2004, **34**, 254–265.
186 G. Juarez-Martinez, *Encyclopedia of Nanotechnology*, 2012, pp. 1235–1248.
187 C. J. Gerdts, G. L. Stahl, A. Napuli, B. Staker, J. Abendroth, T. E. Edwards, P. Myler, W. Van Voorhis, P. Nollert and L. J. Stewart, *J. Appl. Crystallogr.*, 2010, **43**, 1078–1083.
188 M. Maeki, S. Yoshizuka, H. Yamaguchi, M. Kawamoto, K. Yamashita, H. Nakamura, M. Miyazaki and H. Maeda, *Anal. Sci.*, 2012, **28**, 65.
189 D. S. Khvostichenko, J. M. Schieferstein, A. S. Pawate, P. D. Laible and P. J. Kenis, *Cryst. Growth Des.*, 2014, **14**, 4886–4890.
190 S. Guha, S. L. Perry, A. S. Pawate and P. J. Kenis, *Sens. Actuators, B*, 2012, **174**, 1–9.
191 S. Nitahara, M. Maeki, H. Yamaguchi, K. Yamashita, M. Miyazaki and H. Maeda, *Analyst*, 2012, **137**, 5730–5735.
192 M. R. Thorson, S. Goyal, B. R. Schudel, C. F. Zukoski, G. G. Zhang, Y. Gong and P. J. Kenis, *Lab Chip*, 2011, **11**, 3829–3837.
193 M. Maeki, H. Yamaguchi, M. Tokeshi and M. Miyazaki, *Anal. Sci.*, 2016, **32**, 3–9.
194 F. Pinker, M. Brun, P. Morin, A.-L. Deman, J.-F. Chateaux, V. Oliéric, C. Stirnimann, B. Lorber, N. Terrier, R. Ferrigno and C. Sauter, *Cryst. Growth Des.*, 2013, **13**, 3333–3340.

195 T. Tokuhisa, M. Kawasaki, D. Kisailus, M. Yuda, T. Matsunaga and A. Arakaki, *Cryst. Growth Des.*, 2015, **15**, 4549–4555.
196 J. L. Smith, R. F. Fischetti and M. Yamamoto, *Curr. Opin. Struct. Biol.*, 2012, **22**, 602–612.
197 M. Maeki, S. Yoshizuka, H. Yamaguchi, M. Kawamoto, K. Yamashita, H. Nakamura, M. Miyazaki and H. Maeda, *Anal. Sci.*, 2012, **28**, 65.
198 B. Zheng, C. J. Gerdts and R. F. Ismagilov, *Curr. Opin. Struct. Biol.*, 2005, **15**, 548–555.
199 M. Heymann, A. Opthalage, J. L. Wierman, S. Akella, D. M. Szebenyi, S. M. Gruner and S. Fraden, *IUCrJ*, 2014, **1**, 349–360.
200 T. Kojima, S. Onoue, N. Murase, F. Katoh, T. Mano and Y. Matsuda, *Pharm. Res.*, 2006, **23**, 806–812.